Research article

Sensor-less insertion strategy for an eccentric peg in a hole of the crankshaft and bearing assembly

Jianhua Su, Hong Qiao, Zhicai Ou and Yuren Zhang
Institute of Automation, Chinese Academy of Sciences, Beijing, China

Abstract
Purpose – The purpose of this paper is to give a novel sensor-less manipulation strategy for the high-precision assembly of an eccentric peg into a hole.
Design/methodology/approach – Based on the authors' previous work on the attractive region, this paper proposes the sensorless eccentric peg-hole insertion strategy. The analysis is based on the visible strategic behaviors by decomposing the high-dimensional configuration space of the eccentric peg-hole into two low dimensional configuration subspaces. Then, the robotic manipulations can be designed in the configuration subspaces. Finally, a typical industry application, fitting an eccentric crankshaft into a bearing hole of the automotive air-conditioners, is used to validate the presented strategy.
Findings – The attractive region constructed in the configuration space has been applied to guide the robotic manipulations, such as, the locating and the insertion.
Practical implications – The designed robotic assembly system without using force sensor or flexible wrist has an advantage in terms of expense and durability for the automotive air-conditioners manufacturing industry.
Originality/value – Most previous work on sensorless manipulation strategy has concentrated on inserting a symmetric peg into a hole. However, for the assembly of an eccentric peg into a hole, the robotic manipulations should be explored in a high-dimensional configuration space as the six-DOFs of the eccentric peg. In this paper, the decomposition method of the high-dimensional configuration space would make the system analysis visible; then, the assembly strategy can be easily designed in the two subspaces.

Keywords Eccentric peg-in-hole, Robotic assembly, Vision guided, Attractive region, Crankshaft and bearing, Precision engineering, Automotive industry

Paper type Research paper

1. Introduction

Eccentric crankshaft and bearing are the key components of automotive air conditioning compressor. The assembly of the two components is a very important process in the air-conditioners manufacturing industry. The crankshaft is coupled both with an eccentric part, a mid-part and a long-part. The general term "eccentric" refers to the centers of the three parts which are not on the same line. The assembly of the crankshaft and the bearing is to insert the mid-part of an eccentric crankshaft into the inner hole of a bearing. The operation is very important but difficult, as:

- there is a close fit between the mid-part of crankshaft and the hole of bearing; and
- the geometric model of the crankshaft cannot be considered as a cylinder, so, the contact states between the mid-part and the hole are difficult to be predicted.

The eccentric crankshaft and the bearing are shown in Figure 1.

In industry, most manual work was performed in the material handling and packing stations. A robotic system is better at performing high-precision assembly tasks. This is in line with the three groups of automation proposed by Hollnagel (2003). However, the high-precision insertion is difficult to be accomplished by the position adjustment mechanism of a robotic system, and such robotic inaccuracies can possibly lead to uncertainties in gripper position relative to the fixture.

In many situations, robots with sophisticated manipulators require force feedback to achieve the high-precision task. Unfortunately, the high-cost of the initial and maintenance of the sensors are heavy burden for manufacturer, so, in most assembly lines, the tedious work is still done by means of manual operations.

In this study, we aim to design a robotic system to assemble the crankshaft and the bearing without using force sensor or

The current issue and full text archive of this journal is available at **www.emeraldinsight.com/0144-5154.htm**

Assembly Automation
32/1 (2012) 86–99
 [ISSN 0144-5154]
[DOI 10.1108/01445151211198746]

The work was supported in part by the National Natural Science Foundation (NNSF) of China under Grants 60725310 and 61105085. The authors would like to thank Chuankai Liu and Yongkang Luo for their help on the simulations and figures of the manuscript. The authors would also like to thank Junaid Khan for his constructive suggestions, which improved the readability of this paper.

Figure 1 The eccentric crankshaft and bearing

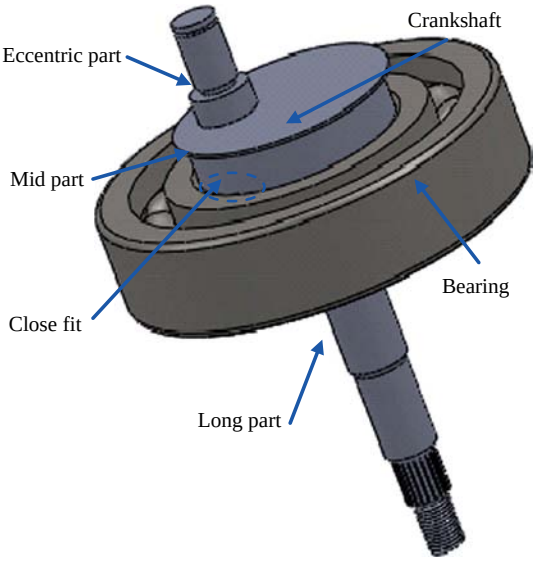

remote center compliance (RCC). The sensor-less assembly strategy to achieve the difficult task is explored based on the attractive region formed in the configuration space.

The previous work on the robotic peg-in-hole insertion is investigated as follows.

1.1 Related works

In many situations, the robotic peg-in-hole insertion is realized by a low-cost RCC or by the guidance of a force sensor.

The utilization of the force sensors in robotic assembly has been widely studied since the 1970s. The studies of Inoue (1974) and Whitney (1982) have been widely recognized as important examples in motion planning. Many other works have applied the assembly methods with a table force sensor or a wrist force sensor. Yao (Yao and Cheng, 1999) derived the geometrical compatibility condition for the insertion motion where mating force/moment were free of overshooting, with an aim to achieve the non-cylinder pairs mating by the aid of force sensors. Zhang (Zhang *et al.*, 2005) modeled the peg-in-hole process as a discrete event system, where the assembly states were recognized with the force information. Tangjitsitcharoen (Tangjitsitcharoen *et al.*, 2009) used a torque sensor to control the position of the shaft during the assembly by setting the limit of torque to stop the motor driver of machine. Shirinzadeh (Shirinzadeh *et al.*, 2010) presented a robotic-based height adjustment method for the assembly of a cylindrical pairs. In their work, the peg-in-hole strategy was established by decreasing the contact forces between the manipulator and the fixture.

The utilization of the flexible wrists and the design principles were analyzed by Whitney and Rourke (1986) and Simunovic (1975). In recent years, over one hundred various devices used in robotic assembly have been developed, such as the dynamic RCC established by Asada and Kakumoto (1988), and the variable remote center compliance (VRCC) developed by Lee (2005). The RCC devices are low cost and reliable for the round peg-in-hole insertions, and have successful industrial applications.

In the robotic peg-hole assembly with sensor feedback, force sensor signal is applied to locate the hole and peg, and then the mapping relationship between the sensory signal and the state of the peg-hole can be obtained. Thus, the robot can adjust the peg to follow the desired trajectory according to the sensory signal. However:

- if the contact surfaces between the peg and the hole are not absolutely smooth, one set of force sensory signal may correspond to many different peg-hole configurations; and
- a small error in relative position or angular position would also make it hard to establish the mapping relationship between the force signal and the peg-hole configurations (Qiao *et al.*, 1996).

The limitations of the RCC are:

- it is no longer useful when there are hundreds of different contact states between the mating parts caused by the position uncertainty of the peg on the gripper (Siciliano and Khatib, 2008); and
- the mating parts must have a chamfer to facilitate the assembly operation (Qiao and Tso, 1998).

Compared with manipulation with sensors and RCC, sensor-less manipulation can provide a simple method to eliminate the uncertainty and can also avoid some problems caused by the force sensors or RCC. The purpose of the sensor-less insertion is to find a region from which the movement with a unique input can lead to the goal makes use of the environment instead of additional devices. In most cases, the uncertainty of the peg-hole in the goal region is less than that in the initial region. In the insertion processing, the constraints formed by the hole can lead the peg move from a relatively large initial region to a relatively small goal region. Thus, the uncertainty elimination can be achieved through the compliant motion because the inputs to the system change with the initial states.

Erdmann's work (Erdmann, 1986; Erdmann and Mason, 1988) formed the fundamental theory of sensor-less manipulation. They investigated the back-projection concept and applied it in sensor-less manipulation strategy investigation. Caine (Caine *et al.*, 1989) carried out research on planar peg-hole insertion operation by analyzing the insertion process from any unknown initial peg-hole configuration to the side-surface contact state without sensor. Matsuno (Matsuno *et al.*, 2004) focused on the problem of inserting a long peg into a tandem shallow hole which was shaped uniquely. They used searched trajectory generation to acquire correct peg posture without feedback. Kilikevicius (Kilikevicius and Baksys, 2011) investigated the process of compliantly supported peg insertion into a bush. In their assembly system, vibratory excitation provided to the bush in the axial direction allowed preventing the balance between the insertion force and frictional forces. Usubamatov (Usubamatov and Leong, 2011) developed a mathematical model for rigid parts with a hole and for the peg clamped in the rigid assembly mechanisms, where the critical angles of the peg's declination and critical depth of the peg's insertion into the hole had also been calculated. In Qiao's work (Qiao *et al.*, 1996, 2002; Qiao and Tso, 1998), the insertion strategies for the round and for the triangular peg-hole systems without force sensors had been proposed. However, in their work, the peg is supposed to be a symmetric regular object, so that, the peg-hole insertion analysis can be visible in three-dimensional spaces.

1.2 The purpose of this paper

One difficulty in sensor-less peg-hole insertion is how to achieve exactness, i.e. how to make sure that the planned path is exactly compliant to the desired contact state, especially when the configuration space of such a contact state is hard to describe analytically due to high dimensionality (Ji and Xiao, 2001). It is a challenge to insert an eccentric peg into a hole where the model of the eccentric peg cannot be considered as symmetry cylinder for custom peg-hole problem. Thus, the motion planning for the eccentric peg-in-hole task needs to be proposed in a high-dimensional configuration space (due to six-DOFs of the eccentric peg).

Based on our previous work on the attractive region, the objective of this paper is to propose a sensor-less insertion strategy in the high-dimensional configuration space, and design a robotic system for the assembly of a crankshaft and a bearing of the automotive air-conditioners. Our analysis is based on visible strategic behaviors by decomposing the high-dimensional configuration space into two low-dimensional configuration subspaces. Then, the robotic manipulations can be designed in the configuration subspaces. And the motion of the eccentric peg should be guaranteed to comply with the desired contacts.

The main works of this paper include:

- A robotic system, including a six-DOF industry robot, a control computer, a pushing device and a camera to identify the target and guide the grasps, is established to assembly a crankshaft and a bearing together.
- A decomposition method is proposed to divide the high-dimensional configuration space into two low subspaces, and the attractive regions in the subspace are analyzed.
- An eccentric peg-in-hole insertion strategy is designed based on the decomposition of the configuration space.

The rest of this paper is arranged as follows: in Section 2, the robotic assembly system is described in detail. In Section 3, the decomposition of the configuration space is explored, and then the attractive regions formed in the high-dimensional configuration space are analyzed. In Section 4, the realization of the insertion strategy is presented. Finally, the whole assembly process is described to show the efficiency of the design strategy and prototype.

2. Develop a robotic system for the assembly of crankshaft and bearing

In this section, a robotic assembly system is designed to accomplish the high-precision insertion task.

The prototype of robotic assembly cell and the sequence of the assembly are designed as follows. It currently consists of four main parts: a Fanuc M6i-B robot, a two-finger gripper to grasp the crankshaft and bearing, a unikon color CCD camera of 704×576 pixels to provide information of the pose of the target, and a device to push the crankshaft into the hole of bearing.

The structure of the robotic system is shown as follows (Figure 2).

2.1 Robot and control computer

The robot chosen for the assembly application is M6i-B. The M6i-B is a six-axis articulated robot, whose repeatability is ± 0.08 mm, and with 6 kg payload. A SMC MHL-16D pneumatic two-finger gripper mounted on the robot is used to pick the crankshaft and bearing. The application programs, such as the motion planning, image processing, are written with Visual C++ software of Microsoft on the control computer. And an ActiveX module, named Fanuc robot I/F, supplies a channel to read/write robot data.

2.2 Image processing unit

The image processing unit used in the assembly system consists of a Unikon color CCD camera for image extraction, and a DS-4002MD image acquisition interface card of Hikvision Company. The camera has 704×576 pixels and 30 images per second. The function of the DS-4002MD is to convert the analog video signal into digital audio and store it in the image memory for control computer processing. The interface card with PCI interface has 32 Kbps-2 Mbps/s image transmission speed. The camera is mounted on the end of the robot, which provides information of the pose of the target. The camera is an "eye" of the robot.

2.3 Pushing device

A practical pushing device that has some means of representing the proposed strategy is designed to insert the crankshaft into the hole. This device is controlled by an AT89S52 microprocessor by driving a motor. The synchronous network communication system between the control computer and the microprocessor of the device consists of a RS232 converter to transfer the feedback of the device and the command of the control computer. The structure of the pushing device is shown in Figure 3.

In the following, the decomposition of the high-dimensional configuration space is presented, and then the attractive regions are constructed in the configuration subspaces.

3. The attractive regions formed in the configuration subspaces of eccentric peg-hole

Owing to the position uncertainties of the gripper and the hole, the crankshaft cannot be moved to the desired state with great precision. In Qiao's work (Qiao *et al.*, 1996; Qiao and Tso, 1998), attractive region was used to eliminate the uncertainty of the symmetry peg state with the aid of constraints from the hole. However, the eccentric peg cannot be supposed as a symmetry object. The rotation uncertainties of the eccentric-part of crankshaft make it difficult to apply the available strategies.

In order to complete the high-precision insertion successfully, a new approach based on attractive region is proposed in the following. The strategy takes the rotation uncertainties of the eccentric-part into consideration.

The concept "attractive region" (Qiao *et al.*, 1996) is briefly introduced below. Assumed that there is a nonlinear system: $dX/dt = f(X, F, t)$, where X is the state of the system, and F is the input to the system. If there is a function $g(X)$, which, for some real number $\varepsilon > 0$, satisfies the following properties: for all X in the region $\|X - X_0\| < \varepsilon$ where X_0 is one state of the system:

- $\begin{cases} g(X) > g(X_0), & X \neq X_0 \\ g(X) = g(X_0), & X = X_0 \end{cases}$;
- $g(X)$ has continuous partial derivatives with respect to all components of X; and
- $dg(X)/dt < 0$.

Therefore, $\|X - X_0\| < \varepsilon$ is an attractive region.

Figure 2 The prototype of robotic assembly cell

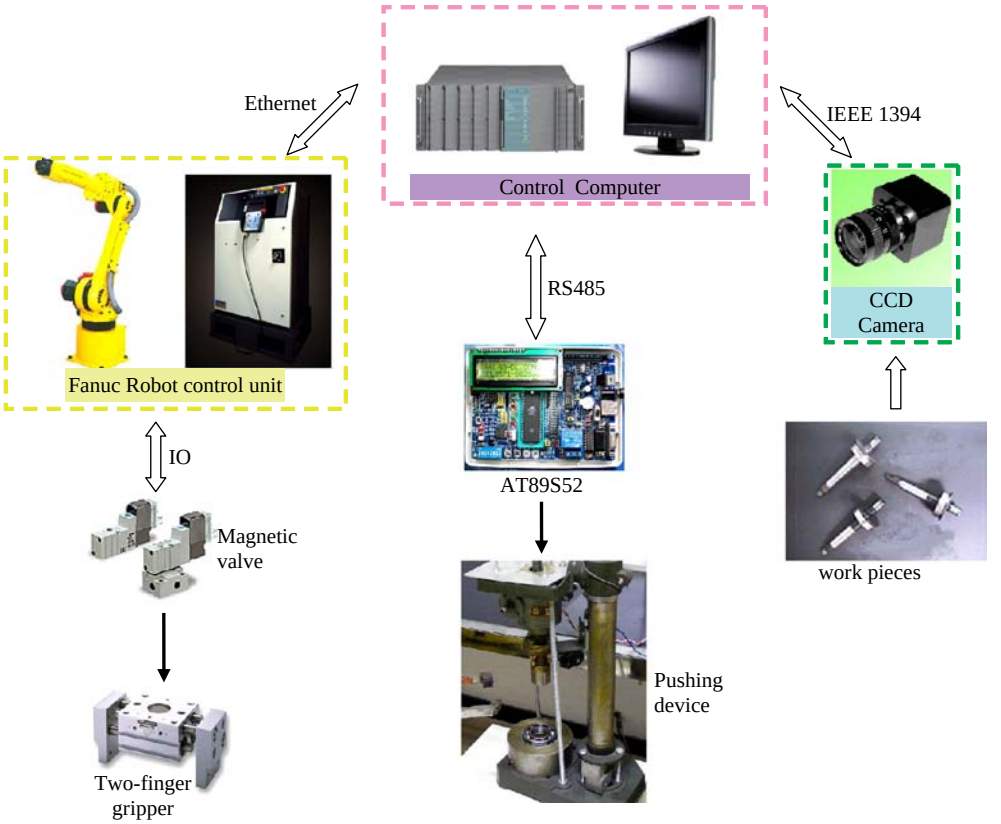

The attractive region gives the description of the object's dynamic motion configurations. In the following, the attractive region formed in the configuration space is analyzed.

3.1 The analysis of configuration space of eccentric peg-hole

In this subsection, the attractive region formed in the configuration space of the eccentric peg-hole system is analyzed first.

There are two coordinate frames used in the analysis of the insertion process:

1 H-coordinate frame is fixed with the hole, where O_h is defined as the centre of the upper-surface of the hole, and O_hY_h is defined as the line from O_h to the robot, O_hZ_h is along the axis of the hole upwards and O_hX_h is perpendicular to O_hY_h and O_hZ_h.
2 C-coordinate frame is fixed with the crankshaft, where O_c is defined as the center of the end-surface of the mid-part, O_cY_c is on the plane passing the axis of the mid-part and the axis of eccentric-part, O_cZ_c is along the axis of the mid-part upwards and O_cX_c is perpendicular to O_cZ_c and O_cY_c.

The pose of the crankshaft in H-coordinate is defined by:

$$X_c = (x_c, y_c, z_c, \beta_c, \alpha_c, \gamma_c)$$

where x_c, y_c, z_c is the position of O_c on H-coordinate, and β_c, α_c, γ_c are the yaw, pitch and roll angle of the crankshaft in H-coordinate. The H-coordinate and C-coordinate are shown in Figure 4.

In Figure 4, the crankshaft has six-DOFs as well as five-DOFs of cylinder peg (the rotation of the cylinder peg around the Z_c-axis can be ignored) in H-coordinate.

Suppose the gravity center of the crankshaft is denoted by O_G. The distance from O_G to the upper surface of hole is denoted by D_G. We define an attractive function as follows:

$$D_G = g(x_c, y_c, \beta_c, \alpha_c, \gamma_c) \quad (1)$$

where x_c, y_c is the position of the crankshaft in H-coordinate, β_c, α_c, γ_c are the yaw, pitch and roll angle of the crankshaft in H-coordinate.

It is hard to design the robotic manipulations in the high-dimensional configuration space (x_c, y_c, β_c, α_c, γ_c, g). In the following, we discuss a method to decompose the high-dimensional configuration space to two low-dimensional configuration subspaces. Therefore, the system analysis becomes visible and the assembly strategy can be easily designed in the two subspaces.

3.2 The decomposition of the configuration space

In this subsection, a method to decompose the configuration space into two low-dimensional subspaces is discussed, so the robotic manipulations can be designed in the two subspaces.

Set $(x_c, y_c, \alpha_c) = (x_c^*, y_c^*, \alpha_c^*)$, where $(x_c^*, y_c^*, \alpha_c^*)$ is treated as constant. Suppose the minimum of $g(x_c^*, y_c^*, \alpha_c^*, \beta_c, \gamma_c)$ is denoted by $g(x_c^*, y_c^*, \alpha_c^*, \beta_c^*, \gamma_c^*)$, as given in equation (2):

$$g(x_c^*, y_c^*, \alpha_c^*, \beta_c^*, \gamma_c^*) = \min_{\beta_c, \gamma_c} g(x_c^*, y_c^*, \alpha_c^*, \beta_c, \gamma_c) \quad (2)$$

Figure 3 The structure of the pushing device

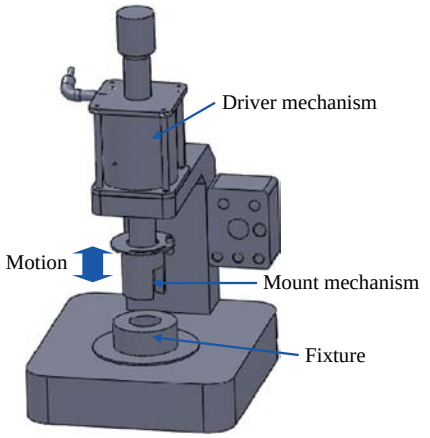

(a)

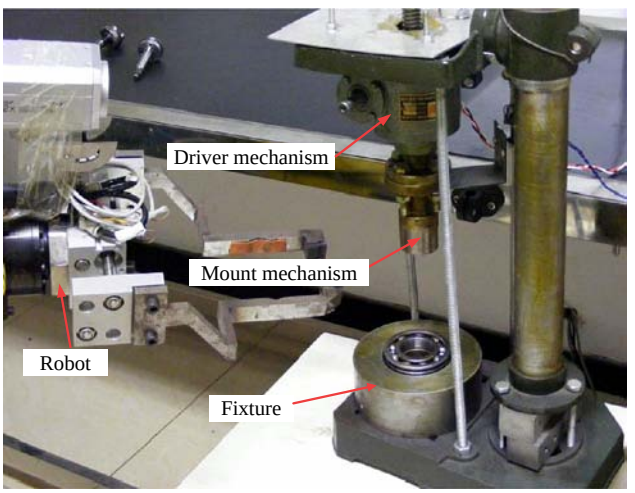

(b)

Notes: (a) CAD model of the pushing device; (b) the real pushing device

Figure 4 The coordinates built on the crankshaft and the bearing

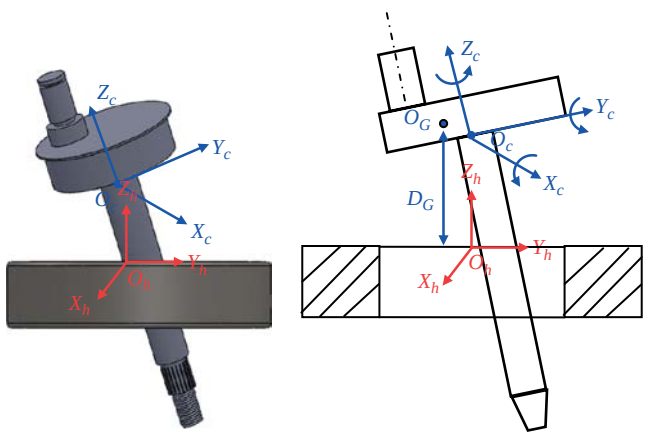

If the configuration space described by $(x_c, y_c, \alpha_c, \beta_c, \gamma_c, g)$ is a convex set, a mapping function can be obtained from equation (2) (Su *et al.*, 2011):

$$t : (\beta_c^*, \gamma_c^*) \rightarrow (x_c^*, y_c^*, \alpha_c^*) \tag{3}$$

The decomposition of configuration space is discussed as follows.

For a constant $(x_c^*, y_c^*, \alpha_c^*)$, when $g(x_c^*, y_c^*, \alpha_c^*, \beta_c, \gamma_c)$ arrives to its minimum, the following equation can be obtained:

$$(\beta_c^*, \gamma_c^*) = t(x_c^*, y_c^*, \alpha_c^*) = (0, 0)$$

If $(x_c^*, y_c^*, \alpha_c^*)$ changes to (x_c', y_c', α_c'), we also can obtain:

$$g(x_c', y_c', \alpha', t(x_c', y_c', \alpha')) = \min_{\beta_c, \gamma_c} g(x_c', y_c', \alpha', \beta_c, \gamma_c)$$

$$(\beta_c', \gamma_c') = t(x_c', y_c', \alpha') = (0, 0)$$

That is, for any fixed (x_c, y_c, α_c), at the minimum of $g(x_c, y_c, \alpha_c, \beta_c, \gamma_c)$, the vector (β_c, γ_c) always equals to zero.

Thus, the configuration space $(x_c, y_c, \alpha_c, \beta_c, \gamma_c, D_G)$ can be decomposed into two low-dimensional subspaces:

1 For a fixed vector $(x_c^*, y_c^*, \alpha_c^*)$, a three-dimensional configuration space is established by:

$$(\beta_c, \gamma_c, D_G)|_{(x_c, y_c, \alpha_c) = (x_c^*, y_c^*, \alpha_c^*)}$$

2 Then, we can keep (β_c, γ_c) at the determined value, and design a set of manipulations to make (x_c, y_c, α_c) arrive to a desired state. The desired state corresponds to the case that crankshaft has been inserted into the hole. The subspace is expressed by:

$$(x_c, y_c, \alpha_c, D_G)|_{(\beta_c, \gamma_c) = (0,0)}$$

3.3 The attractive region formed in the configuration subspace

In this subsection, based on the attractive region formed in the configuration subspaces, the insertion of the crankshaft has been divided into two stages.

Stage 1. In the attractive region formed in the configuration subspace (β_c, γ_c, g), the uncertainties of (β_c, γ_c) can be eliminated by the robotic manipulations designed in the attractive region.

In the following, the attractive regions formed in the subspace $(\beta_c, \gamma_c, D_G)|_{(x_c, y_c, \alpha_c) = (x_c^*, y_c^*, \alpha_c^*)}$ are simulated as shown in Figure 5, where $(x_c^*, y_c^*, \alpha_c^*)$ are selected by different fixed values.

As shown in Figure 5, at the bottom of the attractive region, we can obtain:

$$(\beta_c, \gamma_c) = (0, 0)$$

That is, at the bottom of attractive region, the uncertainties of (β_c, γ_c) would be eliminated. The contact states of eccentric peg-hole and the points on the attractive region formed in the three-dimensional configuration space are shown in Figure 6. Each point inside the region but not on the boundary corresponds to a no-point contact state between the eccentric peg and the hole. Each point inside the region but on the boundary corresponds to a two-point contact state. Each point on the outside surface corresponds to a three-point contact state between eccentric peg and hole. A point on the bottom of the attractive region corresponds to a stable three-point contact state.

Thus, we can use a nominal input which enables the eccentric peg-hole system to follow a nominal trajectory to reach to the local minimum of the attractive region. That is, under the gravity force, the crankshaft can move from no-point contact state to a three-point contact state at the bottom of the attractive region.

Figure 5 The attractive region formed in the configuration subspace $(\beta_c, \gamma_c, D_G)|_{(x_c,y_c,\alpha_c)=(x_c^*,y_c^*,\alpha_c^*)}$

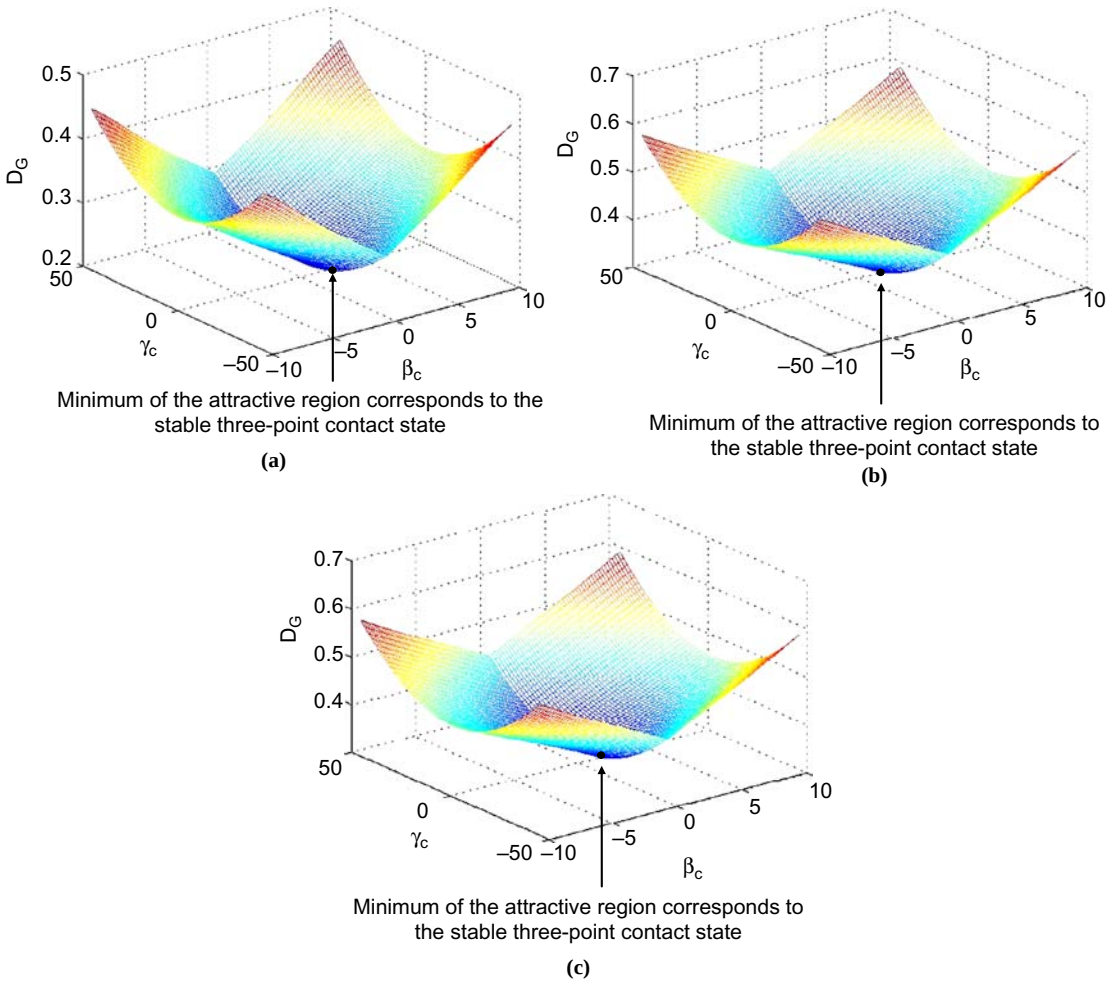

Notes: (a) $(x_c, y_c, \alpha_c) = (0, -0.1, \pi/18)$, the minimum of the attractive region, i.e. $D_G = 0.2228$, is obtained at $(\beta_c,\gamma_c) = (0, 0)$; (b)$(x_c, y_c, \alpha_c) = (0, -0.2, \pi/12)$, the minimum of the attractive region, i.e. $D_G = 0.3263$, is obtained at $(\beta_c,\gamma_c) = (0, 0)$; (c) $(x_c, y_c, \alpha_c) = (0, -0.3, \pi/9)$, the minimum of the attractive region, i.e. $D_G = 0.4145$, is obtained at $(\beta_c, \gamma_c) = (0, 0)$

Stage 2. And then, the uncertainty of (x_c, y_c, α_c) can be eliminated by a pushing force designed in the attractive region formed in subspace $(x_c, y_c, \alpha_c, D_G)$.

At the local minimum of the attractive region, the crankshaft and the hole obtain three-point contact state, where $\alpha_c = \alpha_c^*$, $\beta_c = 0$, $\gamma_c = 0$. In three-point contact state, the geometry center O_G of the crankshaft is on the $Y_hO_hZ_h$-plane. As shown in Figure 7(a), we can obtain:

$$O_GP_2 = O_GP_4$$

The expression denotes that the position uncertainty of the crankshaft along X_h-axis is eliminated. The contact state between the crankshaft and the hole described in the two-dimensional space is shown in Figure 7.

As shown in Figure 7(a) and (b), O_G is the gravity center of the crankshaft. P_1, P_2 and P_4 are the contact points between the hole of the bearing and the mid-part. R is the diameter of the crankshaft. r_1 is the distance from P_3 to O_G. r_2 is the distance from P_1 to O_G. r_3 is the distance from P_2 to O_G.

We define a mapping as below:

$$g_2 : (y_c, \alpha_c) \rightarrow D_G$$

where D_G is the distance from O_G to the upper surface of the hole.

As shown in Figure 8, at the minimum of the graph, we can obtain $(y_c, \alpha_c) = (0, 0)$. That is, an active force F_p can be designed as discussed in Section 4.This force can ensure that the peg-hole keep three-point contact state. And then, it can lead the eccentric peg arrive to the minimum of the attractive region, where the uncertainty of the eccentric peg can be eliminated.

4. Strategy analysis of the eccentric peg-hole insertion

In this section, the realization of the insertion operation is discussed. And, the relationship between the insertion method and the practical manipulations are described by a flowchart shown in Figure 13.

Figure 6 The relationship between the points on the attractive region and the contact states of the eccentric peg-hole

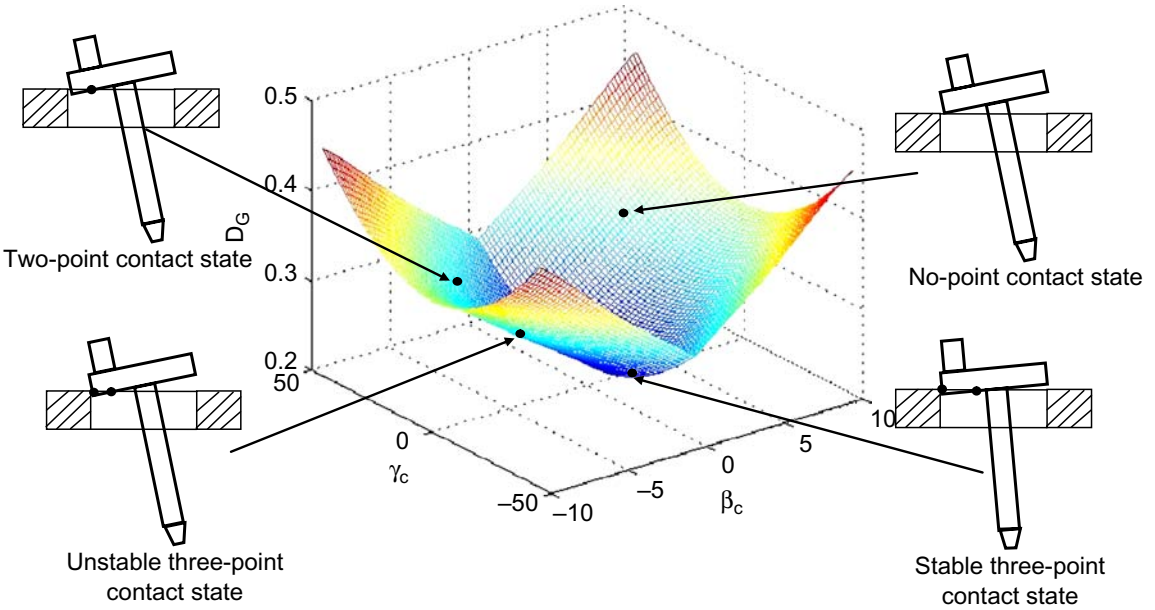

Figure 7 The state of the crankshaft and hole in the two-dimensional space

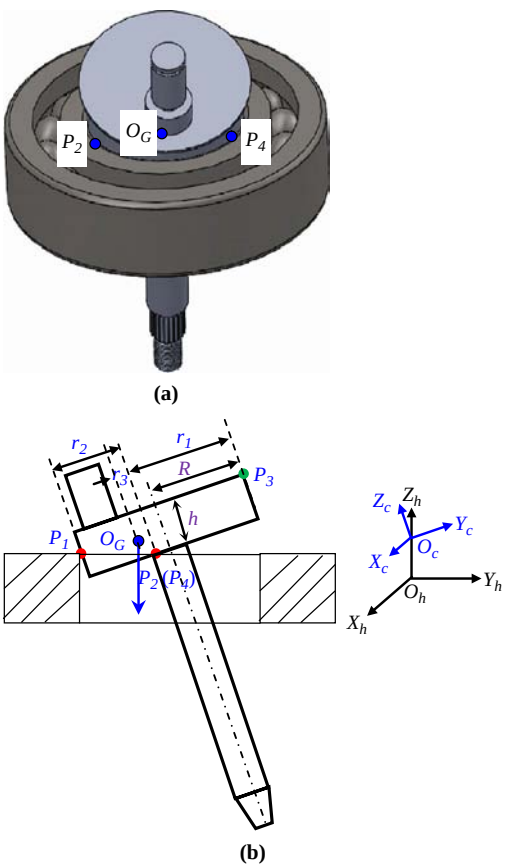

Notes: (a) The state in three-dimensional space; (b) the state in two-dimensional space

4.1 Recognize the target with the aid of vision

Without loss of generality, suppose the height of conveyer is previously known. Thus, the pose of the crankshaft can be described with five-DOF in the conveyor coordinate, as shown in Figure 9.

In Figure 9, G_c is the center of the eccentric-part, G_c' is the projection of G_c. A_c is axis of long part, A_c' is the projection of A_c.

The position of the crankshaft can be described by (α, β, x, y, θ), where α_c is the angle between A_c and A_c', β_c is the rotation angle of crankshaft around A_c. (x, y) is the position of G_c', θ is the direction of A_c' on XOY-plane. When the crankshaft is placed on the plane, its asymmetric geometry always leads it to a stable pose. Thus, the pose parameters to be estimated are (x, y, θ). In the following, the chamfer distance algorithm (Borgefors, 1988) is used for detecting and estimating the three parameters of the crankshaft.

The steps of location of a target crankshaft is shown in Figure 10.

The template matching method is discussed in the following.

Denote the templates of the objects by I_t, $t = 1,2,\ldots,T$ and the image to be detected is I_0. A series of sub-images I_s,$s = 1,2,\ldots,S$ with the same size as I_t are extracted from I_0 successively. The object can be detected by computing the minimum similarity using the Hausdorff distance (Huttenlocher and Klanderman, 1993) measure method:

$$D_{HD} = \min_{s,t} H(I_t, I_s),$$

where $H(I_t, I_s) = \max\{h(I_t, I_s), h(I_s, I_t)\}$ and the function $h(A, B)$ is defined as $h(A,B) = \max_{a\in A} \min_{b\in B} \|a - b\|$.

Then, a brute-force searching is used to estimate the pose space (x, y, θ, s), where s is the scale factor. The matching between the template and the target crankshaft implies its

Figure 8 The attractive region formed in the configuration subspace (y_c, α_c, D_G)

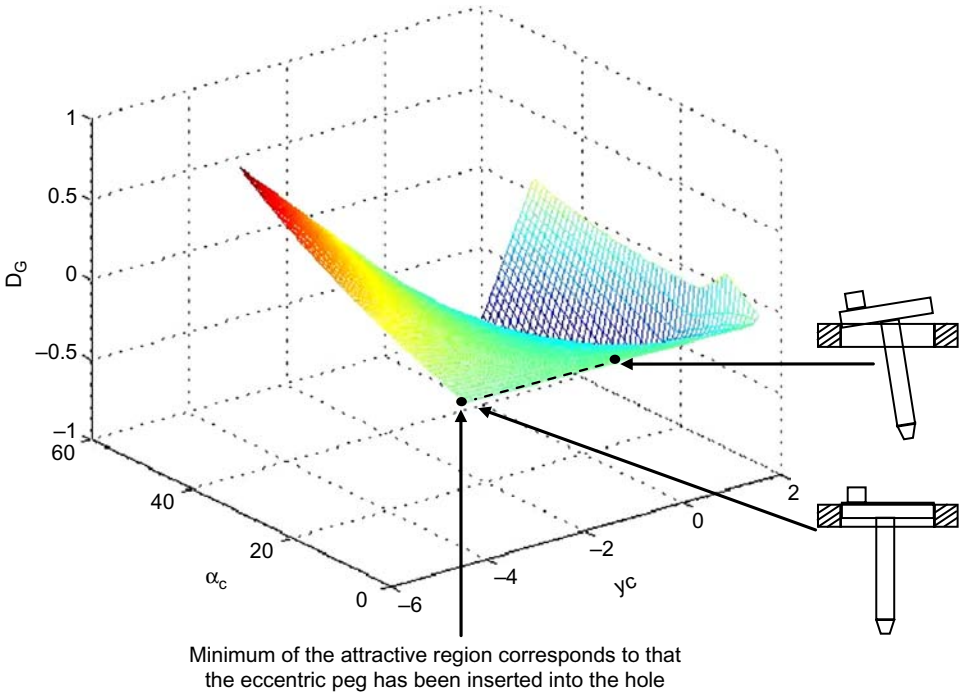

Figure 9 The pose of the crankshaft in the conveyer coordinate frame

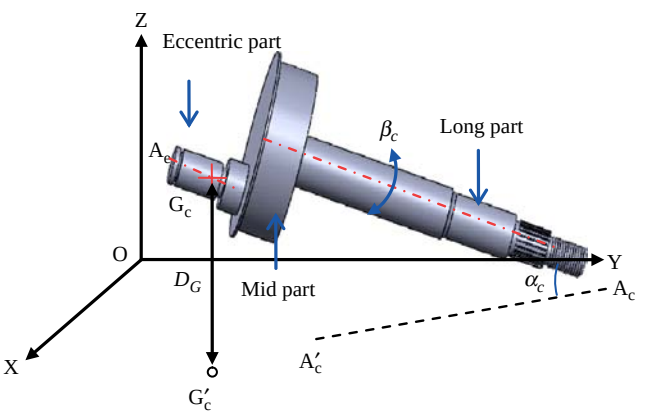

location (x, y) and rotation θ, and thus provides the pose information for grasping.

As the pose of the crankshaft is decided, the gripper can be guided to grasp the crankshaft. The next stage is to eliminate the uncertainty of the eccentric peg with the robotic manipulations and the constraints of the hole.

4.2 Eliminating the uncertainties of (β_c, γ_c) by the robotic manipulations

In this section, we design a set of robot manipulations to eliminate the uncertainty of (β_c, γ_c).

We can use the robot to do the following manipulations:

1 Adjust the orientation of the eccentric peg to (α_c, β_c, γ_c) = (π/9, π/9, π/9).
2 Then, move the eccentric peg to (x_c, y_c) = (0, − 0.3).
3 Finally, put the eccentric peg into the mouth of the hole.

Figure 10 The steps to locate a target crankshaft

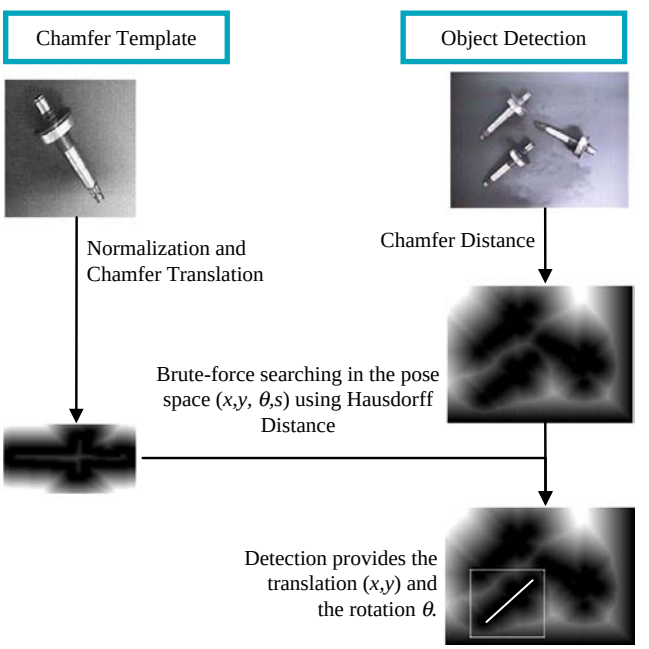

Discussion

The state of the crankshaft held by the gripper cannot be accurately determined at (0, − 0.3, π/9, π/9, π/9), as the pose errors of the gripper and fixture initially.

As analysis in the Section 3, if the state of the crankshaft is in the attractive region formed in the subspace

$(\beta_c, \gamma_c, g)|_{(x_c,y_c,\alpha_c)=(0,-0.3,\pi/9)}$, the crankshaft would converge to the minimum under the gravity force and the contact constraints of the hole. At the local minimum of the attractive region, the uncertainties of the orientation (β_c, γ_c) can be eliminated.

Figure 11 comprises of three figures to show the process of eliminating the uncertainties of the rotation angle (β_c, γ_c).

In the configuration subspace (β_c, γ_c, D_G), the contact states between the crankshaft and hole are analyzed as below.

As shown in Figure 11(a), initially, the crankshaft has been placed on the hole with two-point contact state. In two-contact state, the raw and roll angle of the crankshaft cannot be decided.

In Figure 11(b), the crankshaft has three contact points with the hole. The raw angle equals to zero, i.e. $\beta_c = 0$, which means the uncertainty of the pitch angle is eliminated.

In Figure 11(c), under the gravity force, the crankshaft can approach to the minimum of the attractive region, where the angle $(\beta_c, \gamma_c) = (0, 0)$.

The next step is to eliminate the uncertainties of two related variables (β_c, γ_c).

4.3 Eliminating the uncertainties of (x_c, y_c, α_c) by the pushing device

In this subsection, an inserting force is designed to ensure the crankshaft and the hole keep three-point contact state, and lead the crankshaft arrive to the minimum of the attractive region formed in subspace (y_c, α_c, D_G).The active inserting force F_p can be designed as follows.

The contact forces between the crankshaft and the hole is shown in Figure 12.

As shown in Figure 12(a), F_{sn} is the normal force on the contact point P_1, and F_{st} is the tangential force at P_1. F_{bn} is the normal force on the contact point P_2, and F_{bt} is the tangential force at P_2. F_p is an active force and G is the gravity force.

In the next, the state of the crankshaft under the input force F_p is discussed:

- At initial three-point contact state, the following equations are satisfied:

$$F_p \sin\alpha_c + G\sin\alpha_c = F_{sn} + F_{bt}$$

$$F_p \cos\alpha_c \cdot r_1 - G\sin\alpha_c \cdot r_3 - F_{st}\cdot r_2 = \mathcal{J}\cdot\frac{d\omega}{dt}$$

$$F_{st} < \mu F_{sn}, \quad F_{bt} < \mu F_{bn}$$

$$r_1 = \frac{2R}{1+\cos\alpha_c}$$

$$r_2 = \frac{2R\cos\alpha_c}{1+\cos\alpha_c}$$

  where α_c is the pitch angle and μ is the frictional coefficient between the crankshaft and hole. ω is the angular speed of the crankshaft around P_2. $\mathcal{J}$ is the rotational inertia of the crankshaft.

- Suppose the crankshaft rotates around P_2 with a small angle $\Delta\alpha_c$. Thus, the point P_1 on crankshaft translates along $+Y_p$ direction with T_s:

$$T_s = \frac{r_2}{\cos\alpha_c} - \frac{r_2}{\cos(\alpha_c - \Delta\alpha_c)} > 0$$

  The point P_3 translates along $+Y_p$ direction with T_p:

$$T_p = h[\sin\alpha_c - \sin(\alpha_c - \Delta\alpha_c)] + r_1[\cos(\alpha_c - \Delta\alpha_c) - \cos\alpha_c] > 0$$

Figure 11 The process to eliminate the uncertainties of the rotation angle (β_c, γ_c)

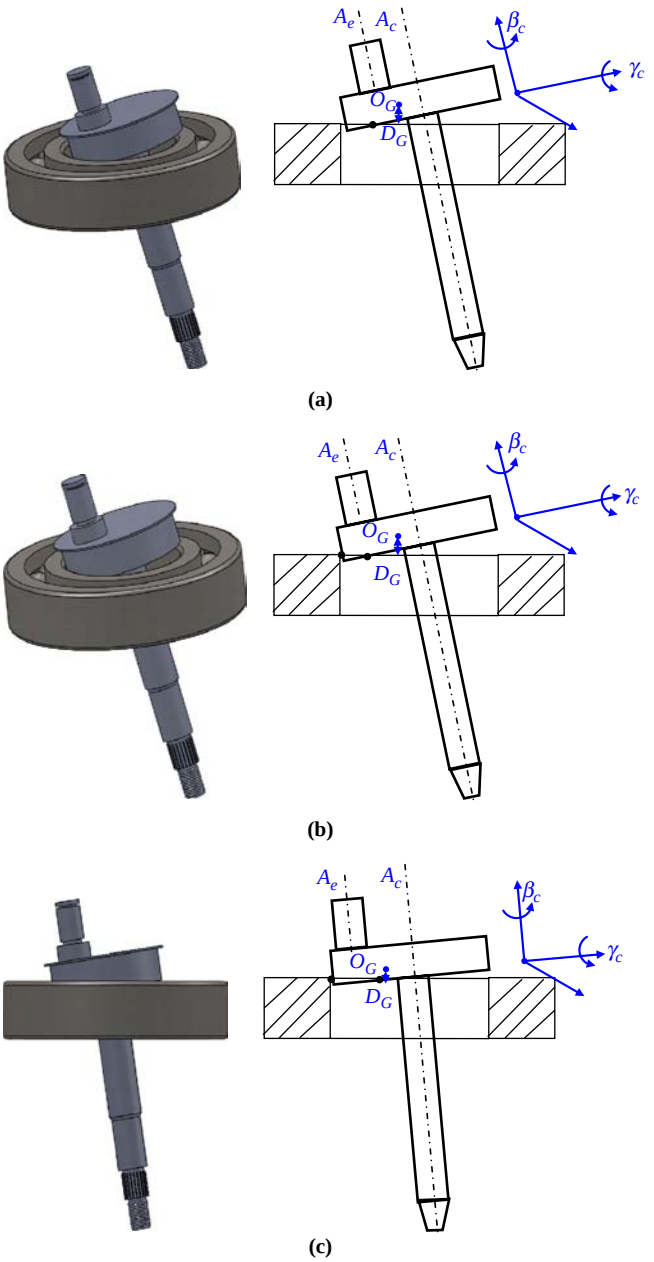

Notes: (a) Two-point contact state; (b) unstable three point contact state; (c) stable three-point contact state

Suppose the point P_2 keeps stationary, and if the translation of P_1 is less than the translation of P_3 along $+Y_p$ direction, i.e. $T_s < T_p$, the point P_1 of crankshaft will leave the hole. Thus, there is only one contact point P_2 between the crankshaft and hole, as shown in Figure 12(a). In this case, the contact forces between the crankshaft and the hole satisfy:

$$F_p \sin(\alpha_c - \Delta\alpha_c) + G\sin(\alpha_c - \Delta\alpha_c) - F_{bt} = -m_p\frac{\Delta v_y}{\Delta t} \quad (4)$$

where v_y is the translational speed along the F_{bt} direction and m_p is the gravity of the crankshaft.

Figure 12 The contact forces between the crankshaft and the hole

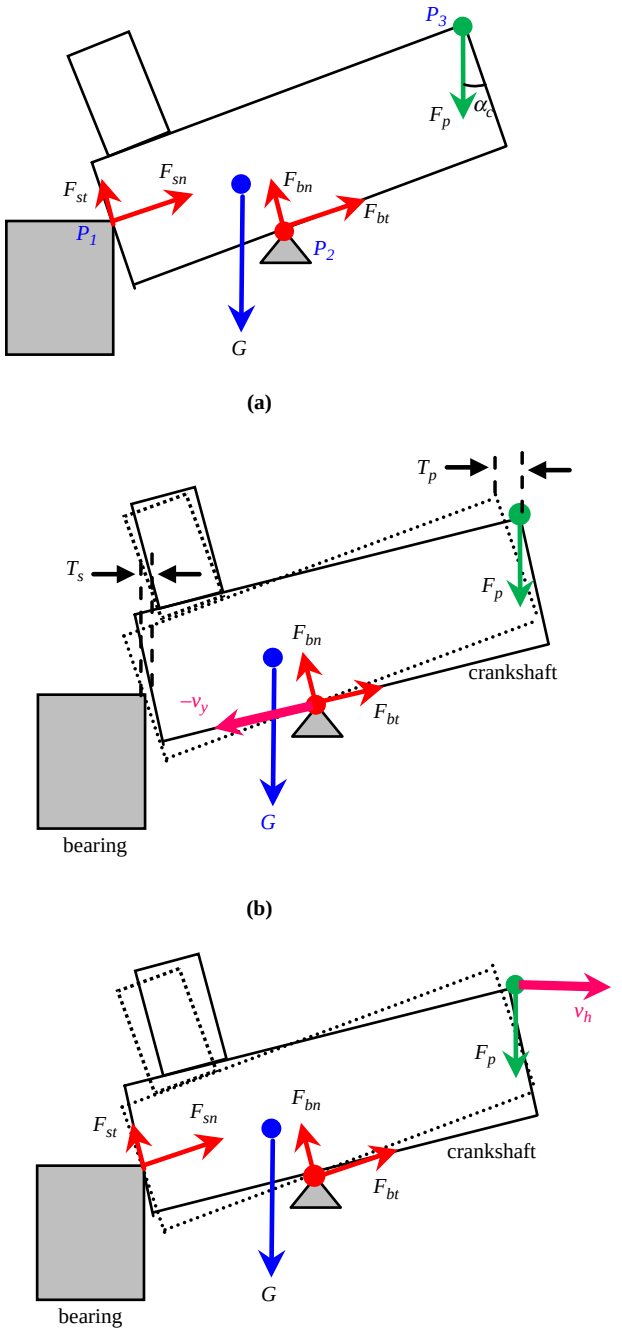

Notes: (a) The forces applied on the crankshaft; (b) the crankshaft and hole contact with two points; (c) the crankshaft and hole keep three point contact

In order to keep the crankshaft in contact with the hole at point P_1 and P_2, the crankshaft should move along $-Y_h$ direction, which needs:

$$\frac{\Delta v_y}{\Delta t} < 0 \tag{5}$$

From equations (4) and (5), we can obtain:

$$F_p \sin(\alpha_c - \Delta\alpha_c) + G\sin(\alpha_c - \Delta\alpha_c) > F_{bt}$$

Also, we can get:

$$\begin{cases} F_p + G > \frac{1}{\sin\alpha_c} F_{bt}, & \alpha_c \neq 0 \\ F_p + G > F_{bn}, & \alpha_c = 0 \end{cases} \tag{6}$$

Expression (6) ensures that the crankshaft and hole keep three-point contact state in the pressing process. Under the pushing forces, the crankshaft would reach to the minimum of the attractive region, which corresponds to the case that the uncertainties of (y_c, α_c) are eliminated.

The initial angle α_c^* in the stage 1 should also satisfy:

$$\alpha_c \leq 2\arcsin\sqrt[3]{\frac{h}{2R}} \tag{7}$$

As discussed in the following, the simplification of T_s and T_p can be expressed by:

$$T_s \approx \frac{r_1 \sin\alpha_c \sin\Delta\alpha_c}{\cos\alpha_c} \tag{8}$$

$$T_p \approx h\cos\alpha_c \sin\Delta\alpha_c + r_1 \sin\alpha_c \sin\Delta\alpha_c \tag{9}$$

The three-point contact state requires the translation of P_1 to be less than the translation of P_2, i.e.:

$$T_s \leq T_p$$

From expressions (8) and (9), one can obtain the expression (7), which ensures that $T_s \leq T_p$. In this case, the crankshaft can be pushed into the hole of the bearing.

Discussion

Function g_2:(y_c, α_c) $\rightarrow D_G$ describes the mapping from state of the crankshaft to the distance D_G.

With the action of the input force and the contact constraints of the hole, D_G should reach to its minimum, which corresponds to a stable state of the crankshaft. That is, the active pushing force should decrease the uncertainties of (y_c, α_c).

As shown in Figure 12(b) and (c), when an active force satisfying expression (4) is applied along $-z_h$ at point P_3, the crankshaft will rotate around point P_2. If the pushing force is suitable, such that it always keeps the three-point contact state as the crankshaft rotates, the distance D_G will be decreased until it achieves minimum value. Finally, the crankshaft can be pushed into the hole of the bearing.

In Figure 13, the manipulations of the robot, such as identifying, grasping and inserting, are described in brief by a flowchart.

In the following, an experimental result from factory is discussed to illustrate our method. And, the explanations of the attractive region and the practical manipulations of the robot and the pushing device are also introduced.

5. Experimental verification

The insertion method based on attractive region outlined above is verified experimentally in this section.

Figure 14 shows the robotic assembly system designed in the Section 2.

Figure 13 The processing of the crankshaft and the bearing assembly

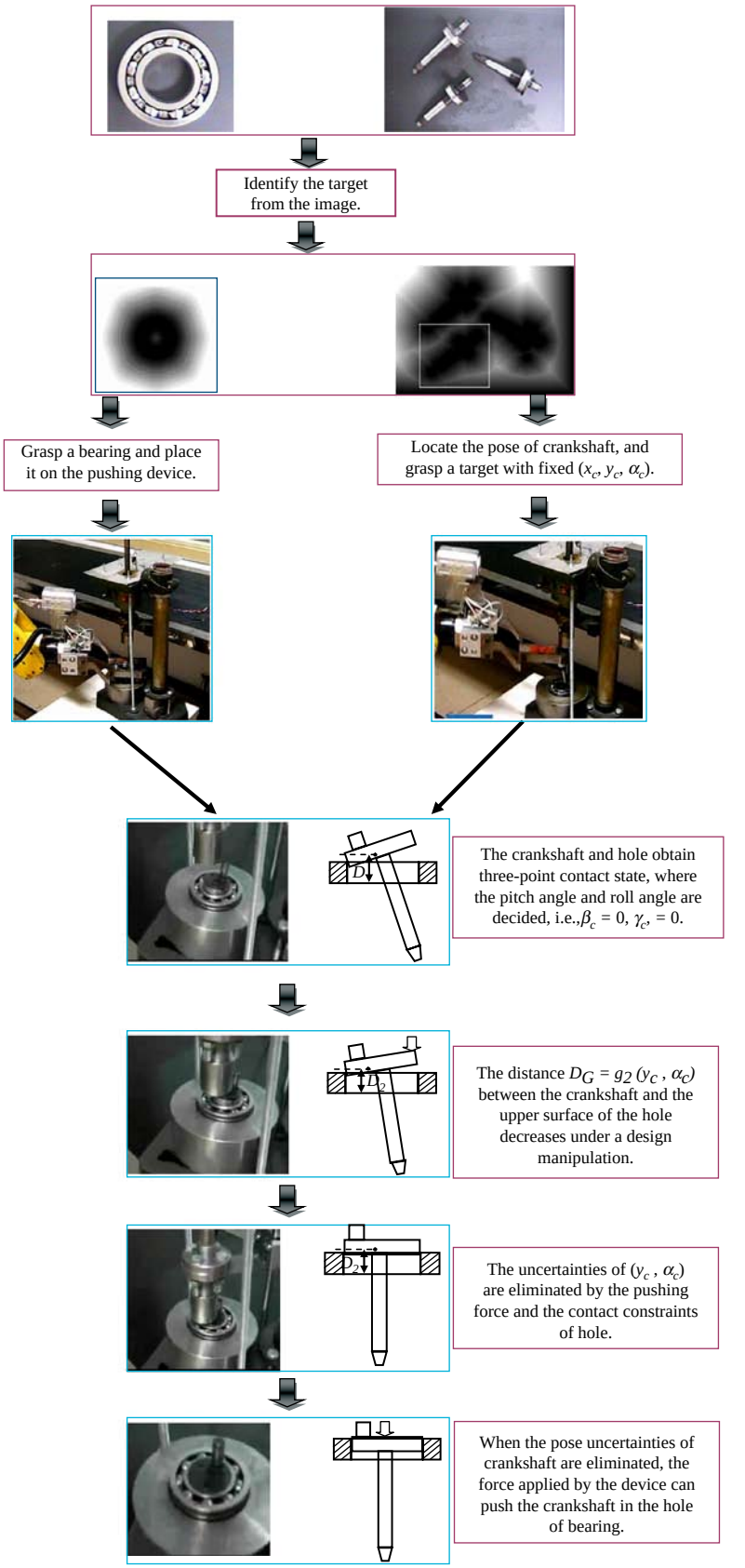

Figure 14 The robotic assembly system

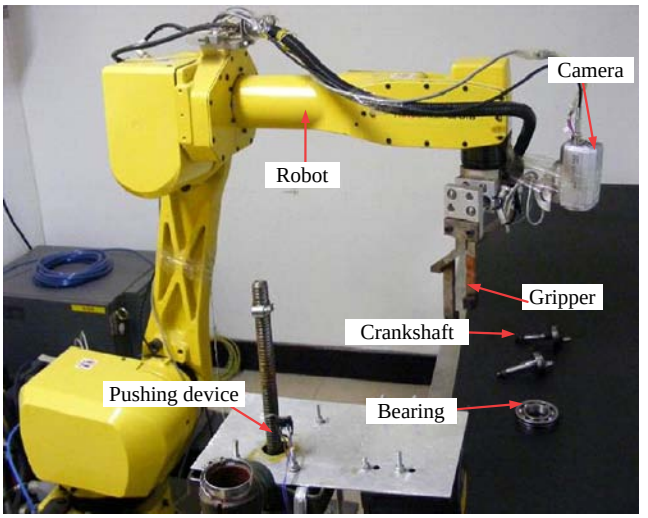

The assembly experiment from factory is discussed in the following.

As shown in Figure 15(a), the camera mounted on the robot scans the conveyor as the robot arm moves above the conveyor, and then the target image is obtained from a set of objects. The input image from the CCD camera is processed in the control computer, and then the pose of the target is transformed from the image coordinate to the robot coordinate. With the aid of visual information, the target crankshaft with the general at an arbitrary place should be identified from a set of parts.

As shown in Figure 15(b), the two-finger gripper should be guided to pick and put a target bearing to the fixture of the pushing device.

As shown in Figure 15(c), the eccentric peg held by the two-finger gripper can be moved from any initial position to the upside of the mouth of the hole. And then, the robot adjust the pose of the eccentric peg to $(x_c, y_c, \alpha_c, \beta_c, \gamma_c) = (0, -0.3, \pi/9, \pi/9, \pi/9)$, which corresponds to a point inside the attractive region formed in configuration subspace (β_c, γ_c, g). Then, the robot puts the crankshaft into the mouth of the hole, and obtains two-point contact state. In this case, under the gravity force, the state of crankshaft would approach to the local minimum of the attractive region. This corresponds to that the uncertainty of orientation (β_c, γ_c) has been eliminated.

As shown in Figure 15(d), in subspace (x_c, y_c, α_c, g), an insertion force satisfying expression (6) can be applied by the mount mechanism of the pushing device. The inserting force can keep three-point contact state and approach to the minimum of the attractive region. This means that the eccentric peg has been inserted into the hole, and the uncertainty of (y_c, α_c) has been eliminated finally.

When the two parts have been fitted together, the robot would pick them out from the pushing device, as shown in Figure 15(e).

Experiments conducted in a factory have shown that the proposed method is sufficient for the high-precision insertion of eccentric peg-hole. We find that the sensor-less method is not sensitive to the environmental contact, e.g. the contact surfaces between the crankshaft and bearing do not have to be absolutely smooth, and the matting part only need a small round corner or a small chamfer to facilitate the assembly. When the initial state of the crankshaft is inside the "mouth" of the attractive region, it would approach to the local minimum by a set of manipulations. Obviously, for bigger crankshaft location and handling error, it would be fail to assembly, because of the crankshaft is outside the attractive region.

Moreover, it is flexible to recognize the position of the crankshafts and the bearings with the aid of vision system. In the experiment, the recognitions of the crankshaft and bearing with occlusions have not been taken into consideration. Further research is needed to improve the performance of recognitions in such a situation.

6. Conclusions

Properly designing of the eccentric crankshaft and bearing robotic assembly system can improve the efficient of the manufacturing of air-conditioner. In this paper, the theoretical and experimental analyses for the assembly of the crankshaft-bearing are given. And a novel sensor-less eccentric peg-in-hole insertion strategy is presented based on the attractive region formed in the configuration space. Thus, a low-cost vision system and pushing device is sufficient to support the high-precision operations of the robot.

Usually, the sensor-less peg-in-hole strategy is explored in a three-dimensional configuration space, where the peg should be regarded as a symmetric part. However, for the insertion of an eccentric peg into a hole, the motion planning should be designed in a six-dimensional configuration space, as the rotation of the eccentric peg cannot be ignored. In this paper, the decomposition method to divide the high-dimensional configuration space into two subspaces (β_c, γ_c, g) and (x_c, y_c, α_c, g). With the aid of the attractive regions formed in the two subspaces, the position and orientation uncertainties of the eccentric peg-hole are eliminated by the designed robotic manipulations.

Figure 15 The practical test of the robotic assembly system in a factory is presented as follows

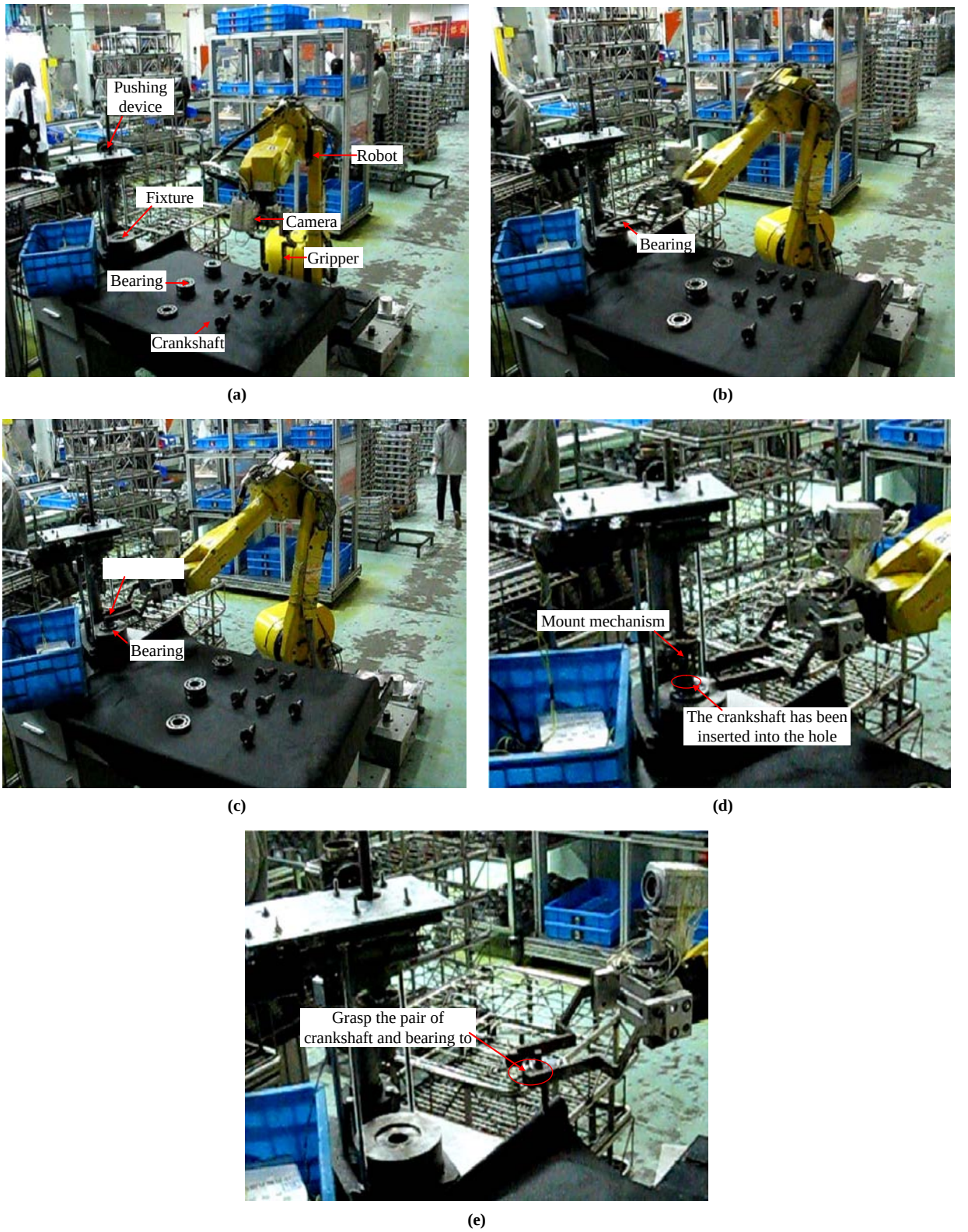

(a) **(b)** **(c)** **(d)** **(e)**

Notes: (a) Identify the pose of the crankshaft and bearing from the worktable;(b) grasp a target bearing and place it on the fixture of the pushing device with a two-finger gripper; (c) grasp and place the crankshaft in the hole of the bearing with fixed ($x_c^*; y_c^*; \alpha_c^*$); (d) push the crankshaft into the bearing by the pushing device; (e) grasp the crankshaftbearing from the pushing device to the shaft

References

Asada, H. and Kakumoto, Y. (1988), "The dynamic RCC hand for high-speed assembly", *IEEE International Conference on Robotics and Automation, Philadelphia, PA*, pp. 120-5.

Borgefors, G. (1988), "Hierarchical chamfer matching: a parametric edge matching algorithm", *IEEE Transactions on Pattern Analysis and Machine Intelligence*, Vol. 10 No. 6, pp. 849-65.

Caine, M.E., Lozano-Perez, T. and Seering, W.P. (1989), "Assembly strategies for chamferless parts", *IEEE International Conference on Robotics and Automation, Scottsdale, AZ*, pp. 472-7.

Erdmann, M.A. (1986), "Using back-projections for fine motion planning with uncertainty", *The International Journal of Robotics Research*, Vol. 5 No. 1, pp. 19-45.

Erdmann, M.A. and Mason, M.T. (1988), "An exploration of sensorless manipulation", *Journal of Robotics and Automation*, Vol. 4 No. 4, pp. 369-79.

Hollnagel, E. (2003), *Handbook of Cognitive Task Design*, Routledge, Mahwah, NJ.

Huttenlocher, D.P. and Klanderman, G.A. (1993), "Comparing images using the Hausdorff distance", *IEEE Transactions on Pattern Analysis and Machine Intelligence*, Vol. 15, pp. 850-63.

Inoue, H. (1974), "Force feedback in precise assembly tasks", AIM 308, Artificial Intelligence Lab MIT, Cambridge.

Ji, X. and Xiao, J. (2001), "Planning motion compliant to complex contact states", *International Journal of Robotics Research*, Vol. 20 No. 6, pp. 446-65.

Kilikevicius, S. and Baksys, B. (2011), "Dynamic analysis of vibratory insertion process", *Assembly Automation*, Vol. 31, pp. 275-83.

Lee, S. (2005), "Development of a new variable remote center compliance with modified elastomer shear pad for robot assembly", *IEEE Transactions on Automation Science and Engineering*, Vol. 2, pp. 193-7.

Matsuno, T., Fukuda, T. and Hasegawa, Y. (2004), "Insertion of long peg into tandem shallow hole using search trajectory generation without force feedback", *IEEE International Conference on Robotics and Automation, New Orleans, LA*, pp. 1123-8.

Qiao, H. (2002), "Strategy investigation with generalized attractive regions", *IEEE International Conference on Robotics and Automation, Washington, DC*, pp. 3315-20.

Qiao, H. and Tso, S.K. (1998), "Strategy investigation of precise robotic assembly operations with symmetric regular polyhedral objects", *Proc. IMechE, Part B: Journal of Engineering Manufacture*, Vol. 212 No. 7, pp. 571-89.

Qiao, H., Moore, P. and Knight, J.A. (1996), "A model and strategy analysis of the peg-hole system associated with robotic assembly operations without chamfers", *International Journal of Robotica*, Vol. 14, pp. 647-58.

Shirinzadeh, B.J., Zhong, Y.M., Tilakaratna, P.D.W., Tian, Y.L. and Dalvand, M.M. (2010), "A hybrid contact state analysis methodology for robotic-based adjustment of cylindrical pair", *International Journal of Advanced Manufacturing Technology*, Vol. 52 No. 4, pp. 329-42.

Siciliano, B. and Khatib, O. (2008), *Springer Handbook of Robotics*, Springer, Berlin.

Simunovic, S. (1975), "Force information in assembly processes", *Proceedings of the 5th International Symposium on Industrial Robots, Bedford, UK*, pp. 415-31.

Su, J.H., Qiao, H., Liu, C.K. and Ou, Z.C. (2011), "A new insertion strategy for a peg in an unfixed-hole of the piston-rod assembly", *International Journal of Advanced Manufacturing Technology*, August (publishing on line).

Tangjitsitcharoen, S., Rojanarowan, N., Tangpornprasert, P. and Virulsri, C. (2009), "Intelligent control of microassembly process based on in-process monitoring of pressing force", *International Journal of Advanced Manufacturing Technology*, Vol. 45, pp. 148-55.

Usubamatov, R. and Leong, K.W.K. (2011), "Analyses of peg-hole jamming in automatic assembly machines", *Assembly Automation*, Vol. 31 No. 4.

Whitney, D.E. (1982), "Quasi-static assembly of compliantly supported rigid parts", *Trans. ASME J. Dynamic Systems, Measurement and Control*, Vol. 104 No. 1, pp. 65-77.

Whitney, D.E. and Rourke, J.M. (1986), "Measurement, and C mechanical behavior and design equations for elastomer shear pad remote center compliances", *ASME J. Dynamic Systems, Measurement and Control*, Vol. 108, pp. 223-32.

Yao, Y.L. and Cheng, W.Y. (1999), "Model-based motion planning for robotic assembly of non-cylindrical parts", *International Journal of Advanced Manufacturing Technology*, Vol. 15, pp. 683-91.

Zhang, W.J., Mao, T.X. and Yang, R.Q. (2005), "A new robotic assembly modeling and trajectory planning method using synchronized Petri nets", *International Journal of Advanced Manufacturing Technology*, Vol. 26 No. 4, pp. 420-6.

Corresponding author

Jianhua Su can be contacted at: jianhua.su@ia.ac.cn